

1 **Constraints on Inner Forearc Deformation From Balanced Cross**  
2 **Sections, Fila Costeña Thrust Belt, Costa Rica**

3

4 Jason C. Sitchler (1), Donald M. Fisher (1), Thomas W. Gardner (2),  
5 and Marino Protti (3)

6

7

8

9 1) Department of Geosciences, The Pennsylvania State University, University Park,  
10 Pennsylvania, USA

11 2) Department of Geosciences, Trinity University, San Antonio, Texas, USA

12 3) Observatorio Vulcanológico y Sismológico de Costa Rica, Apartado 86-3000,  
13 Universidad Nacional, Heredia, Costa Rica

14

15

16 email: sitchler@psu.edu, fisher@geosc.psu.edu, tgardner@trinity.edu, jprotti@una.ac.cr

17

18

## ABSTRACT

19

20

21

22

23

24

25

26

27

28

29

30

31

32

33

34

35

The Fila Costeña thrust belt in the forearc basin of Costa Rica is accommodating a significant portion of the convergence of the Cocos plate and Panama microplate. Geologic mapping of the thrust belt depicts a duplex with three horses that incorporate Eocene limestones and Oligocene-early Miocene clastics inboard of the subducting Cocos Ridge axis. By constructing a cross section at this location along a NE-SW trending transect perpendicular to the thrust belt, we constrain a shortening rate of approximately 40 mm/yr and propose that as much as 50% of the total plate convergence rate is taken up in the inner forearc. The Eocene limestones at the base of the thrust sheets pinch out in both directions away from the onland projection of the Cocos Ridge axis due to decrease in slip on faults and a lateral ramp in the basal decollément. The thrust belt terminates near the Panama border at the onland projection of the subducting Panama Fracture Zone. These observations suggest that shortening is propagating rapidly to the east with the migration of the Panama triple junction and the onset of rapid, shallow subduction of thickened Cocos plate. The absence of similar features in the Nicaraguan forearc where the subducting crust is older, subducts more steeply, and lacks incoming ridges and seamounts, indicates that deformation of the forearc basin in Costa Rica reflects greater coupling inboard of the Cocos Ridge.

36

## Introduction

37           Convergent plate boundaries show a range of behavior with attributes bounded by  
38 two end members: accretionary margins with seaward growth of an accretionary wedge  
39 and erosive margins with basal erosion of a margin wedge and trench retreat [*von Huene*  
40 *and Scholl, 1991; Shreve and Cloos, 1986*]. Erosive margins are typically characterized  
41 by rapid convergence with relatively little sediment input at the trench [*Clift and*  
42 *Vannucchi, 2004*]. They are found in conjunction with recently subducted seamounts and  
43 ridges that increase the degree of coupling between the converging plates [*Norabuena, et*  
44 *al., 2004; Yáñez and Cembrano, 2004*] resulting in forearc deformation, i.e. the  
45 subducting Cocos Ridge beneath the Osa Peninsula in Costa Rica [*Corrigan, et al., 1990;*  
46 *Gardner, et al., 1992; Sak, et al., 2004*), and the New Hebrides and Solomon arcs in the  
47 South Pacific [*Mann, et al., 1998; Taylor, et al., 2005*]. In these cases, the outer forearc  
48 experiences transient uplift and subsidence in response to subducting bathymetric  
49 features.

50           This study focuses on the southeastern end of the Middle America Trench (MAT)  
51 along the Pacific coast of Costa Rica (Figure 1), a region that is considered to be a classic  
52 example of an erosive margin [*Meschede, et al., 1999b; Vannucchi, et al., 2001;*  
53 *Meschede, 2003*]. The interpretation of basal erosion along this margin is supported in  
54 the outer forearc by analysis of slope strata, and benthic foraminifera offshore of the  
55 Nicoya Peninsula to the northwest [*Kimura, et al., 1997; Vannucchi, et al., 2001;*  
56 *Meschede, et al., 2002*] (Figure 2), seismic data [*Hinz, et al., 1996; Ye, et al., 1996*],  
57 high-resolution bathymetry [*von Huene, et al., 1995*], and experimental sandbox models

58 for seamount subduction [*Dominguez, et al., 1998*]. These studies collectively show  
59 active subsidence of the upper slope and arcward retreat of the trench axis.

60 In contrast with the outer part of the forearc, the inner forearc basin in central and  
61 southern Costa Rica is thickened and telescoped by an active thrust system [*Fisher, et al.,*  
62 1998, 2004a]. Additionally, high angle faults, oriented perpendicular to the trench, allow  
63 lateral variations in uplift along the forearc. The areas where the inner forearc exhibits  
64 the most shortening, uplift, and unroofing, lie directly inboard of the areas of greatest  
65 scarring and subsidence related to seamount subduction on the outer forearc [*Fisher, et*  
66 *al., 1998*]. Thus, there is a strong dichotomy between the inner forearc and outer forearc  
67 in the Costa Rican segment of the MAT that directly corresponds with bathymetric  
68 features on the subducting plate. Such a dichotomy between inner forearc shortening,  
69 uplift, and erosion, and outer forearc extension, subsidence, and trench retreat has been  
70 observed along other convergent margins with subducting rough crust such as the New  
71 Hebrides and Solomon island arcs [*Mann, et al., 1998; Meffre and Crawford, 2001;*  
72 *Taylor, et al., 2005*], Japan [*Kodaira, et al., 2000*], and central Chile [*Fisher, et al.,*  
73 2004b; *Kay, et al., 2005; Encinas, et al., 2006*].

74 This raises an important question: What is the mass balance between outer forearc  
75 subsidence and inner forearc uplift? The answer to this question bears on whether  
76 margins such as the Costa Rica MAT experience a transfer of material from the outer to  
77 the inner forearc, or whether they are truly erosional, where material removed from the  
78 margin bypasses the inner forearc. There are two potential mechanisms of inner forearc  
79 thickening along an erosive margin—1) underplating of eroded outer forearc material or  
80 incoming seamounts [*Sak, et al., 2004*], and 2) shortening and duplication by thrusting.



81 Outer forearc erosion has been constrained offshore Nicoya Peninsula with estimates of  
82 subsidence rates related to Late Tertiary to recent erosion [*Vannucchi, et al., 2001*]. The  
83 subsidence rates offshore can be compared with an extensive onland record of Holocene  
84 and Late Quaternary uplift rates and incision rates [*Gardner, et al., 1992; Bullard, 1995;*  
85 *Marshall, et al., 2000; Gardner, et al., 2001; Fisher, et al., 2004a*]. However, it is  
86 difficult to separate the relative contributions of underplating and shortening. Prior to  
87 this study, the inner forearc had been mapped both structurally and stratigraphically using  
88 a combination of aerial photographs and land-based surveys [*Mora, 1979; Lowery, 1982;*  
89 *Phillips, 1983; Kolarsky, et al., 1995; Fisher, et al., 2004a*]. To the best of our  
90 knowledge, there has been only one transect across the inner forearc where the total  
91 crustal thickening and exhumation due to thrusting is estimated [*Fisher, et al., 2004a*],  
92 with no constraints on lateral variations in shortening along the margin.

93         In this paper, we quantify the crustal thickening from thrusting in the inner part of  
94 the Costa Rican forearc system in an area where there are stratigraphic constraints that  
95 allow restoration of thrust-related shortening and characterization of parameters like  
96 shortening rate and the amount of erosional unroofing. The field area lies inboard of the  
97 subducting Cocos Ridge in the Fila Costeña thrust belt, an area that is conjectured to be a  
98 region of strong plate coupling based upon inner forearc shortening, as measured along a  
99 transect near the Río Térraba gorge (Figures 3 and 4, A-A') [*Fisher et al., 2004a*],  
100 geodetic observations in the interseismic period [*Norabuena, et al., 2004; LaFemina, et*  
101 *al., 2005*], and repeated large subduction earthquakes [*Adamek, et al., 1987; Tajima and*  
102 *Kikuchi, 1995*]. We present a geologic map along a 100-km-long segment of the Fila  
103 Costeña thrust belt and evaluate the lateral variations in shortening within the inner

104 forearc in relation to the subducting Cocos Ridge by constructing a new balanced cross  
105 section approximately 25 km east of the Fisher, et al., [2004] transect directly inboard of  
106 the axis of the ridge (Figures 3 and 4, B-B').

### 107 **Regional Tectonic Setting**

108 Costa Rica encompasses the forearc and magmatic arc associated with northeast  
109 subduction of the Cocos plate beneath the Panama microplate along the MAT (Figures 1  
110 and 2). Offshore Nicaragua and western Costa Rica, the northwest domain of the Cocos  
111 crust is characterized by smooth bathymetry, created at the East Pacific Rise 22-24 Ma  
112 [Barkhausen, et al., 2001; Protti, et al., 1995; von Huene, et al., 1995]. Steep subduction  
113 has led to the formation of ridges at low angles to the trench on the outer rise offshore  
114 Nicaragua [Ranero, et al., 2000]. At the Nicoya Peninsula in Costa Rica, rapid  
115 subduction of the smooth Cocos crust corresponds with an active arc system [Alvarado,  
116 et al., 1992; Marshall, et al., 2000; Marshall, et al., 2003; MacMillan, et al., 2004], and  
117 subduction of seafloor sediment [Kimura, et al., 1997]. The southeast domain, created at  
118 the Galapagos rift system 15-16 Ma, is predominately rough crust with a thin sediment  
119 cover and includes several prominent bathymetric features such as the Fisher Seamount  
120 Group (FSG), the Quepos Plateau (QP), and the most expressive feature in the rough  
121 segment of the Cocos plate, the Cocos Ridge (CR) (Figure 2) [Protti, et al., 1995; von  
122 Huene, et al., 1995]. Previous research has shown that this broad, aseismic ridge, which  
123 formed as a result of Galapagos Hot Spot volcanism [Hey, 1977; Werner, et al., 1999],  
124 affects the seismicity [Adamek, et al., 1987; Protti, et al., 1995; Tajima and Kikuchi,  
125 1995], trench-slope morphology [von Huene, et al., 1995], and the style of forearc  
126 deformation in Costa Rica [Corrigan, et al., 1990, Gardner, et al., 1992; Fisher, et al.,

127 2004a]. It is best described as a long wavelength bulge with superposed short  
128 wavelength roughness (e.g. FSG and QP) that subducts slightly obliquely to the trench  
129 and is cut by the subducting Panama Fracture Zone (PFZ).

130         The Central America forearc in Costa Rica can be divided into distinct segments  
131 based on Wadati-Benioff zone geometries [*Protti, et al., 1994*], seismic potential [*von*  
132 *Huene, et al., 2000*], and deformation [*Marshall, et al., 2000*]. Segmentation of the  
133 overriding Panama and Caribbean plates corresponds with lateral variations in subducting  
134 bathymetry. The increase in thickness of subducting crust toward the Cocos Ridge  
135 corresponds with a shift from steep to shallow subduction [*Protti, et al., 1995, 2001*]. In  
136 the northern segment, Wadati-Benioff zone earthquake foci delineate a slab dip of at least  
137 43° whereas a similar section to the south indicates a roughly 19° dipping seismogenic  
138 zone directly inboard of the subducting Cocos Ridge [*Protti, et al., 1995; Norabuena, et*  
139 *al., 2004*]. This change in the dip of the Wadati-Benioff zone indicates a tear or sharp  
140 bend in the seismic slab at depths greater than 70 km, and has been referred to as the  
141 Quesada Sharp Contortion (QSC) [*Protti, et al., 1994; Protti, et al., 1995*]. The QSC also  
142 coincides with the transition on the upper plate from active volcanism in northwestern  
143 Costa Rica to inactive volcanism to the southeast. This volcanic gap, known as the  
144 Cordillera de Talamanca, continues approximately 200 km to the southeast until crossing  
145 the onland projection of the subducting PFZ into western Panama where volcanic activity  
146 resumes [*de Boer, et al., 1991*].

147         The focus of this study is in the region of the forearc that lies above the shallowly  
148 dipping slab between the Cordillera de Talamanca and the Osa Peninsula (Figure 2). The  
149 plate interface beneath this region is strongly coupled [*Adamek, et al., 1987; Norabuena,*

150 *et al.*, 2004], contributing to infrequent, large earthquakes [*Protti, et al.*, 2001;  
151 *Norabuena, et al.*, 2004], such as the April 3, 1983 ( $M_s = 7.3$ ; depth = 30 km) plate  
152 boundary thrust event located beneath the forearc inboard of the Osa Peninsula [*Adamek,*  
153 *et al.*, 1987], and the April 22, 1991 ( $M_s = 7.5$ ; depth = 12 km) back-thrusting event,  
154 located about 100 km to the north beneath the backarc, related to interaction between the  
155 Panama microplate and Caribbean plate [*Tajima and Kikuchi*, 1995]. Segments of the  
156 plate interface adjacent to these coupled regions experience frequent, smaller earthquakes  
157 [*Protti, et al.*, 2001; *Bilek, et al.*, 2003; *Bilek and Lithgow-Bertelloni*, 2005] and outer  
158 forearc subsidence [*Vannucchi, et al.*, 2001].

### 159 **Tectonic Evolution**

160 Changes in subduction geometry, convergence rate and direction, and upper plate  
161 shortening occur at the Panama triple junction where the PFZ subducts beneath the  
162 Panama microplate near the Costa Rica-Panama border. There is an abrupt increase in  
163 subduction angle from west to east across the PFZ, with shallow subduction of the Cocos  
164 plate to the west and steep subduction of the Nazca plate to the east as evidenced by the  
165 presence of active arc volcanism in western Panama [*de Boer, et al.*, 1991]. This  
166 coincides with a sudden change in convergence from nearly orthogonal to highly oblique  
167 subduction and a related decrease in trench-perpendicular convergence rate from ~80  
168 mm/yr to ~20 mm/yr across the subducting PFZ (Figure 5) [*DeMets, et al.*, 1990; *Silver,*  
169 *et al.*, 1990; *Shuanggen, et al.*, 2004]. From NW to SE, the upper plate of the Fila  
170 Costeña abruptly dies out to the southeast, and there is a change from an inactive,  
171 exhumed arc in Costa Rica to an active arc in western Panama (Figure 2) [*Restrepo,*  
172 *1987; de Boer, et al.*, 1988; *de Boer, et al.*, 1991; *MacMillan, et al.*, 2004].

173 Presently, the Panama triple junction migrates to the southeast along the MAT at a  
174 rate of ~55 mm/yr relative to a fixed Panama microplate (Figure 5) [DeMets, *et al.*, 1990;  
175 *Silver, et al.*, 1990; *Shuanggen, et al.*, 2004]. This implies that the upper plate in  
176 southeast Costa Rica experienced slow steep subduction of Nazca crust until the passage  
177 of the triple junction in the last million years. Therefore, the abrupt changes that occur in  
178 the upper plate at the onland projection of the subducting PFZ must migrate eastward into  
179 Panama with eastward migration of the triple junction. There is potential for  
180 complication in this model if the Cocos-Nazca plate boundary jumped in the past 1 m.y.  
181 due to en echelon ridge transform steps associated with the Balboa and Coiba fracture  
182 zones. However, two studies of magnetic anomalies on the Nazca plate examined the  
183 history of these fracture zones (i.e. Miocene-Pliocene westward propagation of fracture  
184 zone activation [*Lonsdale and Klitgord*, 1978; *Lowrie, et al.*, 1979]) and found that the  
185 PFZ has been the active Cocos-Nazca plate boundary for at least the past 1.5 m.y. Based  
186 on this assumption, the PFZ has migrated continuously during the past 1.5 m.y. providing  
187 a time-for-space equivalence along the margin that can be used to determine the time  
188 since onset of deformation at both cross section locations discussed later in this paper.  
189 This is our primary method for determining shortening rates at any given position along  
190 the forearc.

191 In this paper we focus our discussion on the collision of the Cocos Ridge axis, an  
192 event that does not occur until 1-2 Ma according to plate reconstructions when the triple  
193 junction related to the subducting PFZ migrates southeast past the present position of the  
194 ridge [*Lonsdale and Klitgord*, 1978; *Gardner, et al.*, 1992; *MacMillan, et al.*, 2004].  
195 Given that the Cocos Ridge is oriented roughly N44E and the relative convergence vector

196 between the Cocos plate and the Panama block is oriented N30E, the ridge will migrate to  
197 the northwest at a rate of 20 km/Ma (Figure 5). Thus, the axis of the indenting ridge has  
198 not migrated more than 40 km since initial arrival at the MAT.

199       Much of the deformation of the inner forearc in Costa Rica can be attributed to  
200 Cocos Ridge collision along the MAT. Estimates for the timing of arrival of the Cocos  
201 Ridge along the MAT range from 8 Ma [*Abratis and Wörner, 2001*] to 1 Ma [*Lonsdale*  
202 *and Klitgord, 1978; Gardner, et al., 1992*]. The earliest estimate of 8 Ma is based on  
203 cessation of "normal" calc-alkaline magmatism and occurrence of anomalous adakitic  
204 magmatism [*de Boer, et al., 1991; Drummond, et al., 1995*] distributed throughout  
205 southern Costa Rica and into Panama [*Abratis and Wörner, 2001*]. An arrival estimate of  
206 5.5 Ma is derived from fission track ages that indicate rapid unroofing of the arc at this  
207 time [*Gräfe, et al., 2002*]. Benthic foraminifera assemblages suggest emergence of the  
208 forearc and backarc dated at 3.6 and 1.6 Ma, respectively [*Collins, et al., 1995*].  
209 Stratigraphic, paleontological, and structural data on the exposed outer forearc in  
210 southern Costa Rica document Cocos Ridge effects around 1 Ma [*Corrigan, et al., 1990*],  
211 and oceanic crust magnetic anomaly data place the rough crust of the Cocos Ridge at the  
212 MAT 1 Ma in Neogene plate reconstructions [*Lonsdale and Klitgord, 1978; Gardner, et*  
213 *al., 1992; MacMillan, et al., 2004*]. We suggest that the range in estimates for Cocos  
214 Ridge arrival reflects differing definitions of the "ridge", with earliest estimates based on  
215 the arrival of anomalously thick oceanic crust along the northwest flank of the ridge that  
216 was created at the Galapagos rift system, and more recent estimates based on the arrival  
217 of the truncated ridge axis *sensu strictu*.

218

## The Térraba Trough

219           The exposed Tertiary forearc basin in southern Costa Rica has been collectively  
220 referred to as the Térraba Trough [*Yuan, 1984*]. What was once an inner forearc  
221 depositional basin, similar to the present-day submerged, seismically imaged, deep  
222 Sandino basin of Nicaragua [*Ranero, et al., 2000*], is now a thrust faulted coastal  
223 mountain range (i.e., the Fila Costeña) (Figure 2). As in the case of the Sandino basin in  
224 Nicaragua, the strata of the forearc basin in Costa Rica record the depositional history  
225 inboard of the outer forearc rise. In this section, we summarize the mappable formations  
226 used in palinspastic reconstructions of the thrust belt.

227           The Térraba River provides a natural transect through the central portion of this  
228 mountain range and has been a primary location for previous sedimentological [*Mora,*  
229 *1979; Lowery, 1982; Phillips, 1983*], and structural [*Mora, 1979; Kolarsky, et al., 1995;*  
230 *Fisher, et al., 2004a*] surveys. Five distinctive stratigraphic units were identified in the  
231 Fila Costeña. These units, the Brito Formation, Térraba Formation, Curré Formation, an  
232 unnamed Pliocene unit and the Paso Real Formation, are described in terms of five,  
233 respective, margin-scale lithofacies: (1) carbonate-dominated turbidites, (2) mixed  
234 bioclastic and volcanoclastic turbidites to volcanoclastic-dominated turbidites, (3)  
235 volcanoclastic dominated conglomerate and breccia, (4) fossiliferous mudstone and (5)  
236 lahars (Figure 3, inset) [*Mora, 1979; Lowery, 1982; Phillips, 1983*]. The entire  
237 stratigraphic column, as measured in the thrust belt, constitutes more than 4 km of forearc  
238 basin sediments deposited in the last 55 m.y. atop crystalline basement rock [*Phillips,*  
239 *1983; Yuan, 1984*] of the Nicoya Complex, which is only exposed in basement highs

240 related to outer forearc uplift [*Phillips*, 1983; *Yuan*, 1984]. The basement/cover contact  
241 is, therefore, a nonconformity or a faulted unconformity [*Phillips*, 1983; *Yuan*, 1984].

242 The Brito Fm. is the oldest sedimentary unit exposed in the Fila Costeña.

243 Although the lower contact is not exposed in the thrust belt, it is presumed that the  
244 carbonate sequence in southeastern Costa Rica is approximately 600 m thick and rests  
245 atop the Nicoya Complex [*Phillips*, 1983]. The Térraba Fm., named after the type  
246 locality along the Río Térraba of Costa Rica, conformably overlies the Brito Fm. This  
247 Oligocene to Lower Middle Miocene mixed bioclastic/volcaniclastic turbidite sequence  
248 consists of approximately 1000 m of black shale, marl, sandstone, and conglomerate.  
249 The formation, in a broad sense, becomes increasingly coarse and volcaniclastic toward  
250 the top, suggesting a regional shoaling during this time period associated with the  
251 development of the Central American arc complex [*Phillips*, 1983]. Gabbroic intrusions,  
252 dated by K-Ar at 15 – 11 Ma, intrude both the Brito Fm. and Térraba Fm. [*de Boer, et al.*,  
253 1995; *MacMillan, et al.*, 2004].

254 As the depositional environment shoaled adjacent to the volcanic arc during the  
255 Middle and Late Miocene, the deposits became progressively more conglomeratic. This  
256 gradation into a shallow marine and terrestrial environment marks the base of the Curré  
257 Fm., which generally coarsens upward and includes approximately 830 m of  
258 volcaniclastic sediment. The top of the formation is poorly exposed, but in at least two  
259 locations in the central and northwest Fila Costeña, an unnamed Pliocene mudstone, up to  
260 200 m thick and dated using fossil evidence, rests unconformably upon the terrestrial  
261 sediments of the Upper Curré Fm, [*Kesel*, 1983] indicating a final marine inundation  
262 before inner forearc basin deformation and exhumation [*Kesel*, 1983]. Terrestrial alluvial



263 deposits (i.e. lahars, pyroclastics, and lava flows) of the Pliocene Paso Real Fm. were  
264 subsequently shed off of the Cordillera de Talamanca into the forearc, forming another  
265 regional unconformity [*Kesel*, 1983; *Phillips*, 1983]. The unnamed marine mudstone was  
266 not found in our mapping area and is assumed to have largely been removed prior to  
267 deposition of the Paso Real Formation [*Kesel*, 1983]. Therefore, the unconformity  
268 between the Curré and Paso Real Fms. and the correlative unconformity between the  
269 unnamed Pliocene mudstone and the Paso Real Fm. provides a maximum age for the  
270 onset of exhumation in the Fila Costeña. Consequently, we can calculate an absolute  
271 minimum long term shortening rate for the thrust belt.

272         The Quaternary deposits found in the vicinity of the Fila Costeña are regionally  
273 unconformable and can broadly be divided into the mid Pleistocene to Holocene Brujo  
274 Fm. [*Phillips*, 1983] (located outside of our map area) and unnamed recent terrace  
275 gravels. The Brujo Fm. is composed of alluvial fan and debris flow deposits shed off of  
276 the Cordillera de Talamanca into the valley between the Cordillera de Talamanca and the  
277 Fila Costeña [*Kesel*, 1983] to the northwest of our map area. In the 1970's, Richard Kesel  
278 identified several features indicative of active, ongoing uplift and exhumation of the  
279 Cordillera de Talamanca and inner fore arc. These include faulted and back-tilted  
280 alluvial fans, lacustrine deposits formed from stream reversals, radiocarbon dated at 9 and  
281 13 ka, and the appearance and increase in relative abundance of Cordillera de Talamanca  
282 – sourced plutonic clasts in the middle and upper Brujo Fm., above a 26.5 ka radiocarbon  
283 dated sample [*Kesel*, 1983].

284         Incised fluvial terraces are preserved along rivers that cross the thrust belt, and the  
285 elevation of Late Quaternary terraces near the thrust front requires uplift along the frontal

286 thrust [Bullard, 1995; Murphy, 2002; Fisher, et al., 2004a]. Dated marine terraces are  
287 also observed along the frontal thrust in the central Fila Costeña [Fisher, et al., 2004a].  
288 In the region of the thrust belt directly inboard of the Cocos Ridge axis, extensive  
289 landslides have been shed off of the topographic divide (Figures 3 and 6). An individual  
290 slide in this region has an area of 39 square kilometers (Figure 3). Today, these deposits  
291 are identified by vegetated, hummocky topography that extends at least 4 km from the  
292 steep divide and contains limestone boulders in excess of several meters in diameter.

### 293 **Geologic and Structural Mapping of the Fila Costeña**

294 The Fila Costeña is a 20-30 km wide thrust belt that extends approximately 250  
295 km from the Golfo de Nicoya to the Panama border. The geology of the southern ~2,000  
296 sq. km was mapped using 1:50,000 topographic base maps (Figure 3). The mapped area  
297 encompasses the southeastern portion of the deformed Tertiary forearc basin inboard of  
298 the Cocos Ridge. Outcrops are generally limited to coastal headlands, numerous valley  
299 walls and streambeds oriented perpendicular to the structure, and quarries. The thrust  
300 belt in this area is comprised of three to five continuous thrust slices that imbricate the  
301 Térraba Trough. Strata within imbricate thrust slices strike parallel to the MAT (WNW-  
302 ESE) and dip ~15° – 35° to the northeast. Mesoscale folds associated with southwest-  
303 directed thrusts in the thrust belt verge seaward with subhorizontal axes parallel to thrust  
304 traces. Overturned beds are rare but can be locally observed in the footwall of major  
305 thrusts.

306 The major thrusts are most easily recognized in our map area where they place  
307 carbonates of the Brito Fm. on top of turbidites of the Térraba Fm. The Brito Fm.,  
308 therefore, provides a key bed that is used to line length balance cross sections (Figure 4).

309 To the northwest of our map area, the central Fila Costeña lies inboard of relatively  
310 smooth subducting bathymetry on the northwest flank of the subducting Cocos Ridge.  
311 Here, the frontal thrust steps offshore, parallels the coastline, and returns landward along  
312 a lateral ramp [Fisher, *et al.*, 2004a]. No limestone is exposed at the base of the thrust  
313 faults in this region, indicating a décollement above the Brito Fm. at the northwest extent  
314 of the mapped area in this study (Figure 3).

315 As the thrust belt nears the onland projection of the Cocos Ridge axis to the  
316 southeast, the basal décollement deepens stratigraphically toward the basement/cover  
317 contact, as indicated by the presence of Brito Fm. limestone at the base of the individual  
318 thrusts. Slightly off-axis to the west, three thrusts expose hanging wall flats within the  
319 limestone and a fourth thrust at the rear of the thrust belt exposes a hanging wall flat  
320 stratigraphically higher in the Térraba Fm. (Figure 4, A-A'). Directly inboard of the  
321 subducting Cocos Ridge axis, the total number of thrust sheets increases from three to  
322 five (Figure 4, B-B'). This imbricate fault system could be described as either an  
323 imbricate fan or a duplex. The observation that the frontal three thrust sheets are thinner  
324 than the total thickness of the Térraba Trough as defined by the depth-to-detachment  
325 (Figure 4, inset) at the rear of the thrust belt requires that, either 1) the Térraba Trough  
326 was significantly thinner to the southwest in the case of an imbricate fan, or 2) the frontal  
327 thrust slices involve only the deeper strata of the Térraba Trough and the roof thrust of a  
328 duplex is eroded away. We favor a duplex model because the basal limestones on thrust  
329 faults 2a and 2b terminate laterally at hanging wall cutoffs before merging at leading  
330 branch lines (Figure 3).

331           In the area where thrust shortening is greatest, the topographic divide is roughly  
332 1,700 m high, at least 200 m higher than the top of the divide along strike (Figure 6).  
333 This divide is supported by massive limestones uplifted by thrust fault #3 (Figures 3 and  
334 4, B-B'). Recent landslides scour the unstable southwest-facing slope. Hummocky  
335 topography extends approximately four kilometers to the southwest away from the divide  
336 between fault #3 and fault #2b (Figure 3). This is the only location within the  
337 southeastern Fila Costeña where there is evidence of extensive landslides on the order of  
338 tens of square kilometers.

339           Total shortening decreases northwest and southeast of this region as individual  
340 thrusts merge at leading branchlines with the roof thrust. Farther to the east, the thrust  
341 belt terminates, or shortening is greatly reduced, across north-south trending tear faults  
342 that extend to the north into Pleistocene deposits [*Cowan, et al., 1997; Morell, et al.,*  
343 2005]. These right-lateral faults coincide with the updip projection of the PFZ and have  
344 been interpreted as indentation faults that are deeply rooted in the crust of the Panama  
345 microplate [*Kolarsky, et al., 1995*].

346           The overall regional pattern within the thrust belt is a lenticular culmination that  
347 exposes basal limestones in a series of laterally tapering thrust slices centered over the  
348 axis of the subducting ridge (Figure 3). This trend of decreasing shortening to the  
349 northwest is also suggested by the absence of Brito Fm. in thrusts (i.e. stepping-up of the  
350 decollément into younger strata). To quantify this relationship, two balanced cross  
351 sections were constructed: one along the Térraba gorge along a transect described by  
352 *Fisher, et al. [2004a]* and another within the culmination inboard of the Cocos Ridge axis  
353 where the shortening is inferred to be the greatest (Figure 4). To the southeast of both of

354 these transects, the thrust belt ends abruptly near the Costa Rica-Panama border at the  
355 updip projection of the subducting PFZ (Figures 2 and 3).

356         Balanced cross sections were constructed using structural data collected in the  
357 field throughout the Tertiary and Quaternary deposits in the southeast Fila Costeña thrust  
358 belt. Toward the rear of the thrust belt, the axial surface related to the closing bend at the  
359 base of frontal footwall ramps is placed behind the rearmost observation of steeply  
360 dipping strata in order to both minimize shortening and satisfy dip data at the surface.  
361 This axial surface is projected to the intersection with the rearmost thrust that exposes  
362 Brito Fm. along the base. This fault in cross section is constrained by the surface trace  
363 and the dip of beds in the hanging wall. Based on these assumptions, the decollément  
364 depth is at approximately 3500 and 4000 m below the surface, a depth that is in  
365 agreement with previous structural and stratigraphic studies in the nearby Térraba gorge  
366 [*Phillips, 1983; Fisher, et al., 2004a*].

367         The Fila Costeña is depicted in these cross sections as a thin-skinned thrust belt  
368 with imbricate faults that are rooted at the basement-cover contact. We base this  
369 interpretation on the observation that, for most exposed thrusts within the area, the  
370 hanging wall consists of a flat at or near the base of the Brito limestone. In one such case  
371 we have measured the orientation of a regional fault surface and associated slickenlines, a  
372 fault that places Brito Fm. atop Térraba Fm., and with dip slip on a surface that strikes  
373 N70W and dips 45 degrees to the northeast. In six other cases we measured less  
374 extensive faults with strikes ranging from N79W to N24W (average = N52W) and dips  
375 from 19 to 54 degrees NE (average = 40 degrees). Slickenlines measured on these six  
376 fault surfaces plunge an average of 25 degrees with vergence of S21W, indicating

377 primarily dip slip motion. Fold trends at five locations range from N88W to N15W  
378 (average = N64W). These observations, coupled with the absence of any exposed  
379 basement in the mapping area, are consistent with low angle thrusting that detaches the  
380 sedimentary cover from the Nicoya Complex with southwestward vergence.

381         Based on a line-length balance of the Brito Fm. on a cross section located above  
382 the subducting axis of the Cocos Ridge, the minimum slip is 4.5 km, 5.5 km, 6.3 km, 8.1  
383 km, and 12 km for faults 1, 2a, 2b, 3, and 4, respectively, representing a minimum  
384 shortening of approximately 36 km, a 58% decrease in line length (Figure 4, B-B').  
385 Using the distance from the onland projection of the PFZ (~50 km) as a proxy for time  
386 since the onset of deformation (~1 Ma), this indicates a shortening rate of nearly 40  
387 mm/yr, roughly half of the Cocos-Panama plate convergence rate of ~80 mm/yr (Figure  
388 5). The lateral equivalent of fault #4 in section B-B' was not included in the cross section  
389 in *Fisher, et al.*, [2004a], because this fault does not expose the Brito Fm. in the Térraba  
390 gorge. On the map, the fault is required by the exposure of a Brito Fm. hanging wall  
391 cutoff along the fault just to the southeast of the gorge (Figure 3, "HW Cutoff"). To the  
392 east of this exposure, shallow dip measurements in the Térraba Fm. indicate a hanging  
393 wall flat. Therefore, the addition of this fault in that section increases the overall  
394 shortening from 17 km to approximately 33 km, or 55% total shortening (Figure 4, A-A').  
395 Although both reconstructions minimize the shortening, the cross section near the  
396 Térraba gorge exposes hanging wall cutoffs in two of the thrust sheets (Figure 4, A-A').  
397 Therefore, the potential to underestimate the shortening is less likely at that location than  
398 at the center of the culmination where most of the Brito cutoffs are eroded (Figure 4, B-  
399 B').

## Discussion

400

401           The observations we present in this paper illustrate that accommodation of active  
402 convergence occurring at a convergent plate boundary may rapidly shift from the trench  
403 to the inner forearc in response to increased outer forearc coupling, such as shallow  
404 subduction of thickened crust [von Huene, *et al.*, 1995]. In the case of southeastern Costa  
405 Rica, the inner forearc is accommodating upper plate shortening between the extinct arc  
406 and the MAT. The deformation is localized in the region affected by the colliding Cocos  
407 Ridge, with rates of shortening roughly 50% of the total Cocos-Panama convergence rate.  
408 This increase in coupling in conjunction with relatively fast subduction of young oceanic  
409 crust is contrary to model results for quasi-static equilibrium [Yáñez and Cembrano,  
410 2004], indicating that the features we observe represent a transient response to Cocos  
411 Ridge subduction.

412           The Fila Costeña thrust belt of Costa Rica records a minimum of 36 km of slip on  
413 five major thrust faults directly inboard of the axis of the subducting Cocos Ridge. Tear  
414 faults in the thrust belt are restricted to lateral ramps as the decollement cuts up section to  
415 the northwest [Fisher, *et al.*, 2004a] and to the southeast above the onland projection of  
416 the subducting PFZ. For estimates of shortening, we assume that the thrust faults record  
417 primarily dip slip, an observation that is consistent with measured slickenlines along the  
418 exposed faults in the area, including one major fault.

419           It should be noted that we were not able to locate any observable outcrop of the  
420 Curré Fm. in the frontal portion of the Fila Costeña southeast of the Terraba gorge. The  
421 depositional facies associated with the Curré Fm. must have been confined to the region  
422 proximal to the volcanic arc and paleoshoreline. We speculate that this depositional

423 environment did not exist at the restored location of the front of the thrust belt, some 80  
424 km away from the volcanic arc, during the time of deposition of the Curré Fm. The  
425 correlative facies at that distal location would be more similar to that of the Térraba Fm.,  
426 and a Curré-type sequence may never have been deposited there. This would imply that  
427 the undeformed basin had trenchward variations in lithofacies and would display  
428 significant disparities in post-compaction thicknesses, a conjecture that is consistent with  
429 seismic reflection data landward of the outer forearc rise in the deep Sandino basin of  
430 Nicaragua [Ranero, *et al.*, 2000], with seaward thinning of sedimentary packages relative  
431 to a forearc basin depocenter. Given the discontinuous nature of exposure in the thrust  
432 belt, we employ the simplest case for structural reconstruction, which is to consolidate  
433 the Térraba Fm. and Curré Fm. on the maps and cross sections, and assume a constant  
434 basin-wide thickness for each sedimentary unit based on measurements made in the  
435 Térraba gorge during previous studies [Phillips, 1983]. This is a simplification that bears  
436 no relevance on our minimum shortening estimate that is based on conservation of line  
437 length for the base of the Brito Formation. Nevertheless, seaward thinning of units would  
438 have a large effect on the geometry of the thrust system in cross sections and the position  
439 of the roof thrust in reconstructions.

440 Radiocarbon dated volcanoclastics of the Brujo Fm. that are faulted and back-  
441 tilted, and lacustrine deposits formed from stream reversals as a result of this tilting  
442 [Kesel, 1983] as well as incised Quaternary river terraces [Bullard, 1995; Murphy, 2002;  
443 Fisher, *et al.*, 2004a] indicate that the Fila Costeña is actively deforming. Where the  
444 thrust belt extends offshore, there is a regionally extensive marine platform that indicates  
445 uplift rates of 0.34 mm/yr and 1.5 mm/yr [Fisher, *et al.*, 2004a]. The map and cross



446 sections of the Fila Costeña show that shortening in the inner forearc is greatest inboard  
447 of the Cocos Ridge axis, where the thrust belt assembles into a duplex, and decreases  
448 along-strike. This unique structural feature within the thrust belt lies directly in front of  
449 the highest and sharpest topographic divide in the Fila Costeña (Figures 3 and 6), a ridge  
450 that is supported by resistant limestones that comprise the rear thrust in the duplex.  
451 Landslides are shed off of the divide and bury strata on the backside of the adjacent thrust  
452 sheet to the south (Figure 3). Major thrusts inboard of the Cocos Ridge axis detach at  
453 the contact between the crystalline basement rock and the overlying Tertiary forearc  
454 basin sequence, producing a duplex that imbricates the lower strata of the Térraba basin.  
455 Several of the fault traces merge laterally, away from the onland projection of the ridge  
456 axis, as the duplex terminates to the northwest and southeast at leading branch lines. As  
457 the overall number of faults decrease, they step upsection from the basement/cover  
458 contact into the Térraba Fm. These observations support conjectures that shallow  
459 subduction of the Cocos Ridge has caused arching of the Panama microplate parallel to  
460 the plate convergence vector [*Corrigan, et al., 1990; Kolarsky, et al., 1995*]. If this is the  
461 case, the depth of the basal detachment beneath the thrust belt relative to some horizontal  
462 datum may be constant, while shallowing stratigraphically to the east and west due to  
463 basement arching above the Cocos Ridge axis [*Kolarsky, et al., 1995*].

464 Current geodetic observations using a limited GPS array can be used to infer the  
465 coupling between the Cocos plate and the Panama microplate [*Norabuena, et al., 2004*].  
466 However, these tools typically measure displacements related to elastic strains that  
467 accumulate during the interseismic part of the seismic cycle rather than long-term, time-  
468 averaged deformation rates. *Norabuena, et al., [2004]* describe GPS displacements from

469 a regional network in Costa Rica that depict greater coupling in the area inboard of the  
470 subducting Cocos Ridge than in other parts of the thrust belt. A single site within the  
471 area of the thrust culmination of the Fila Costeña records an arcward velocity of ~35  
472 mm/yr relative to a stable Caribbean plate [Norabuena, *et al.*, 2004], a value that is very  
473 close to our estimate for long term shortening rates. The map and cross sections of this  
474 study indicate that the increased plate boundary coupling inferred for the interseismic  
475 time period are matched by greater amounts of long-term upper plate shortening in the  
476 inner forearc.

### 477 **Conclusions**

478 There is an active thrust belt along the Central American convergent margin that  
479 uplifts the inner forearc basin in Costa Rica. Geologic maps and cross sections lead to  
480 several conclusions about the relationship between the Cocos plate and Panama  
481 microplate at the MAT in southeastern Costa Rica. 1) Deformation is concentrated  
482 inboard of the Cocos Ridge where a culmination is reached by an imbricate stack with an  
483 eroded roof thrust. 2) This region coincides with a relative increase in interseismic  
484 coupling based on geodetics [Norabuena, *et al.*, 2004]. 3) The total number of thrusts  
485 decreases to the northwest and southeast of the onland projection of the Cocos Ridge axis  
486 where they join adjacent thrusts at leading branch lines, indicating erosion through the  
487 roof thrust in the area of greatest shortening. Away from the Cocos Ridge axis, the  
488 decollément of the Fila Costeña steps up laterally into the Térraba Fm. 4) To the  
489 southeast, the topographic expression of the thrust belt ends abruptly at the onland  
490 projection of the subducting PFZ, suggesting that the thrust belt may be actively  
491 propagating to the southeast with the Panama triple junction. 5) Minimum shortening

492 within the thrust belt since the middle Pliocene is 36 km, representing more than 58%  
493 shortening in the inner forearc. 6) The calculated minimum shortening rate of ~40 mm/yr  
494 inboard of the Cocos Ridge axis represents nearly 50% of the total plate convergence  
495 rate. 7) Given shortening rates of 10's of mm's per year along the Fila Costeña, much of  
496 the trench retreat estimated for the outer forearc (e.g., *Vannucchi, et al.*, [2004]) can be  
497 accounted for by increased plate boundary coupling and underthrusting of the outer  
498 forearc wedge beneath the inner forearc.

499

### **Acknowledgements**

500

This research was supported by the National Science Foundation (EAR-0337456)

501

along with funding from the P.D. Krynine Memorial Fund from the Penn State University

502

Department of Geosciences. The paper benefited from reviews by E. Kirby and R.

503

Slingerland, and three additional anonymous reviewers.

## References

- 504  
505  
506 Adamek, S., et al. (1987), Seismic rupture associated with subduction of the Cocos  
507 Ridge, *Tectonics*, 6, 757-774.  
508  
509 Abratis, M., and G. Wörner (2001), Ridge collision, slab-window formation, and the flux  
510 of Pacific asthenosphere into the Caribbean realm, *Geology*, 29, 127-130.  
511  
512 Alvarado, G. E., et al. (1992), Chronostratigraphy of Costa Rican Igneous Rocks Based  
513 on Radiometric Dating, *J. South Am. Earth Sci.*, 6, 151-168.  
514  
515 Bilek, S. L., and C. Lithgow-Bertelloni (2005), Stress changes in the Costa Rica  
516 subduction zone due to the 1999 Mw=6.9 Quepos earthquake, *Earth Plan. Sci. Let.*, 230,  
517 97 – 112.  
518  
519 Bilek, S. L., et al. (2003), Control of seafloor roughness on earthquake rupture behavior,  
520 *Geology*, 31, 455-458.  
521  
522 Bird, P. (2003), An updated digital model of plate boundaries, *Geochem. Geophys.*  
523 *Geosys.*, 4.  
524  
525 Bullard, T. F. (1995), Neotectonics, geomorphology, and late Quaternary geology across  
526 a forearc region impacted by the subduction of the aseismic Cocos Ridge, Pacific coast of  
527 Costa Rica, Ph.D., 775 pp., Univ. of N.M., Albuquerque, N.M., USA.  
528  
529 Clift, P., and P. Vannucchi (2004), Controls on tectonic accretion versus erosion in  
530 subduction zones: Implications for the origin and recycling of the continental crust, *Rev.*  
531 *Geophys.*, 42.  
532  
533 Collins, L. S., et al. (1995), Timing and rates of emergence of the Límón and Bocas del  
534 Toro basins: Caribbean effects of Cocos Ridge subduction?, *Spec. Paper, Geol. Soc.*  
535 *Amer.*, 295, Mann, P., 263-289.  
536  
537 Corrigan, J., et al. (1990), Fore-Arc Response To Subduction Of The Cocos Ridge,  
538 Panama Costa-Rica, *Geol. Soc. Amer. Bull.*, 102, 628-652.  
539  
540 Cowan, H., et al., (1997), Active faulting at the Cocos-Nazca-Caribbean Plate triple  
541 junction, southern Costa Rica and western Panama, *Abstracts with Programs, Annual*  
542 *Meeting, Geol. Soc. Amer.*, 29, 442.  
543  
544 de Boer, J. Z., et al. (1988), Quaternary calc-alkaline volcanism in western Panama;  
545 regional variation and implication for the plate tectonic framework, *J. South Amer. Earth*  
546 *Sci.*, 1, 275-293.  
547  
548 de Boer, J. Z., et al. (1991), Evidence For Active Subduction Below Western Panama,  
549 *Geology*, 19, 649-652.

550  
551 de Boer, J. Z., et al. (1995), Cenozoic magmatic phases of the Costa Rican island arc  
552 (Cordillera de Talamanca), *Spec. Paper, Geol. Soc. Amer.*, 295, Mann, P., 35-55.  
553  
554 DeMets, C., et al. (1990), Current Plate Motions, *Geophys. J. Int.*, 101, 425-478.  
555  
556 Dominguez, S., et al. (1998), Upper plate deformation associated with seamount  
557 subduction, *Tectonophysics*, 293, 207-224.  
558  
559 Encinas, A., et al. (2006), Finding of a Holocene marine layer in Algarrobo (33°22'S),  
560 central Chile. Implications for coastal uplift, *Revista Geológica de Chile*, 33, 2, 339-345.  
561  
562 Fisher, D. M., et al. (1998), Effect of subducting sea-floor roughness on fore-arc  
563 kinematics Pacific coast, Costa Rica, *Geology*, 26, 467-470.  
564  
565 Fisher, D. M., et al. (2004a), Active thrusting in the inner forearc of an erosive  
566 convergent margin, Pacific coast, Costa Rica, *Tectonics*, 23, TC2007, doi:  
567 10.1029/2002TC001464.  
568  
569 Fisher, D. M., et al. (2004b), In the Footsteps of Charles Darwin: Patterns of Coastal  
570 Subsidence and Uplift Associated with Seamount Subduction, Basal Fore-Arc Erosion  
571 and Seamount Accretion in Latin America, paper presented at AGU, Fall Meeting, edited,  
572 AGU, San Francisco, Calif., USA.  
573  
574 Fisher, M. A., et al. (1991) Structure of the collision zone between Bougainville guyot  
575 and the accretionary wedge of the New-Hebrides island-arc, southwest Pacific, *Tectonics*  
576 10, 887-903.  
577  
578 Gardner, T. W., et al. (1992), Quaternary Uplift Astride The Aseismic Cocos Ridge,  
579 Pacific Coast, Costa-Rica, *Geol. Soc. Amer. Bull.*, 104, 219-232.  
580  
581 Gardner, T. W., et al., (2001), Holocene Fore Arc Deformation in Response to Seamount  
582 Subduction, Peninsula de Nicoya, Costa Rica, *Geology*, 29, 151-154.  
583  
584 Gräfe, et al., (2002), Geodynamic evolution of southern Costa Rica related to low-angle  
585 subduction of the Cocos Ridge: constraints from thermochronology, *Tectonophysics*, 348,  
586 187-204.  
587  
588 Hare, Paul W. and T.W. Gardner (1985), Geomorphic indicators of vertical tectonism  
589 along converging plate margins, Nicoya Peninsula, Costa Rica, ch. 4, *in* Tectonic  
590 Geomorphology, Proceedings of the 15th Geomorphology Symposia Series, Binghamton,  
591 NY, pp. 76-104.  
592  
593 Hey, R. N., (1977), Tectonic evolution of the Cocos-Nazca spreading center, *Geol. Soc.*  
594 *Amer. Bull.*, 88, 1404-1420.  
595

596 Hinz, K., et al. (1996), Tectonic structure of the convergent Pacific margin offshore Costa  
597 Rica from multichannel seismic reflection data, *Tectonics*, 15, 54.  
598  
599 Hovius, N., et al. (1998), Landslide-driven drainage network evolution in a pre-steady-  
600 state mountain belt: Finisterre Mountains, Papua New Guinea, *Geology*, 26, 1071-1074.  
601  
602 Kay, S. M., et al. (2005), Episodic arc migration, crustal thickening, subduction erosion,  
603 and magmatism in the south-central Andes, *Geol. Soc. Amer. Bull.*, 117, 67-88.  
604  
605 Kesel, R. H. (1983), Quaternary history of the Rio General Valley, Costa Rica, *Res. Rep.*  
606 *Natl. Geog. Soc.*, 15, Oehser, P. and Lea, J., 339-358.  
607  
608 Kimura, G., et al. (1997), Proceedings of the Ocean Drilling Program; Initial reports;  
609 Costa Rica accretionary wedge; covering Leg 170 of the cruises of the drilling vessel  
610 JOIDES Resolution, San Diego, California, to Balboa, Panama, sites 1039-1043, 16  
611 October-17 December 1996, 458 pp., *Tex. A & M Univ., ODP*, College Station, Tex.,  
612 USA.  
613  
614 Kodaira, S., et al. (2000), Subducted seamount imaged in the rupture zone of the 1946  
615 Nankaido earthquake, *Science*, 289, 104-106.  
616  
617 Kolarsky, R. A., et al. (1995), Island arc response to shallow subduction of the Cocos  
618 Ridge, Costa Rica, *Spec. Paper, Geol. Soc. Amer.*, 295, Mann, P., 235-262.  
619  
620 LaFemina, P. C., et al. (2005), Subduction of an Aseismic Ridge: Interseismic  
621 Deformation Above the Cocos Ridge, Costa Rica, *Eos Trans. AGU*, 86(52), Fall Meet.  
622 Suppl., Abstract T42A-07.  
623  
624 Lallemand, S. E., et al. (1992), Reconstruction Of Subduction Zone Paleogeometries And  
625 Quantification Of Upper Plate Material Losses Caused By Tectonic Erosion, *J. Geophys.*  
626 *Res.*, 97, 217-239.  
627  
628 Lonsdale, P., and K.D. Klitgord (1978), Structure and tectonic history of the eastern  
629 Panama Basin, *Geol. Soc. Amer. Bull.*, 89, 981-999.  
630  
631 Lowery, B. J. (1982), Sedimentology and Tectonic Implications of the Middle to Upper  
632 Miocene Curre Formation, Southwestern Costa Rica, B.S., La. St. Univ., Baton Rouge,  
633 La., USA.  
634  
635 Lowrie, A., et al., (1979) Fossil spreading center and faults within the Panama fracture  
636 zone, *Mar. Geophys. Res.*, 4, 153-166.  
637  
638 MacMillan, I, et al., (2004) Middle Miocene to present plate tectonic history of the  
639 southern Central American Volcanic Arc, *Tectonophysics*, 392, 325-348.  
640  
641 Mann, P., et al. (1998), Accelerating late Quaternary uplift of the New Georgia Island

642 Group (Solomon island arc) in response to subduction of the recently active Woodlark  
643 spreading center and Coleman seamount, *Tectonophysics*, 295, 259-306.  
644  
645 Marshall, J. S., et al. (2000), Central Costa Rica deformed belt: Kinematics of diffuse  
646 faulting across the western Panama block, *Tectonics*, 19, 468-492.  
647  
648 Marshall, J. S., et al. (2003), Landscape evolution within a retreating volcanic arc, Costa  
649 Rica, Central America, *Geology*, 31, 419-422.  
650  
651 Meffre, S., and A. J. Crawford (2001), Collision tectonics in the New Hebrides arc  
652 (Vanuatu), *Island Arc*, 10, 33-50.  
653  
654 Meschede, M., et al. (1999a), Subsidence and extension at a convergent plate margin:  
655 evidence for subduction erosion off Costa Rica, *Terra Nova*, 11, 112-117.  
656  
657 Meschede, M., et al. (1999b), Melange formation by subduction erosion: the case of the  
658 Osa melange in southern Costa Rica, *Terra Nova*, 11, 141-148.  
659  
660 Meschede, M. (2003), The Costa Rica convergent margin: a textbook example for the  
661 process of subduction erosion, *Neues Jahrbuch Fur Geologie Und Palaontologie-*  
662 *Abhandlungen*, 230, 409-428.  
663  
664 Mora, C. R. (1979), Estudio geologico de una parte de la region sureste del Valle del  
665 General, Provincia Puntarenas, Costa Rica, undergrad. thesis, 185 pp., Universidad de  
666 Costa Rica, San Pedro, Costa Rica.  
667  
668 Morell, K., et al., (2005), Forearc Deformation, Arc Volcanism, and Landscape Evolution  
669 near the Cocos-Nazca-Caribbean Triple Junction, *Eos Trans., AGU*, 86(52), Fall Meet.  
670 Suppl., Abstract T24A-05.  
671  
672 Murphy, K. (2002), Use of weathering rinds in fluvial terrace correlation along the  
673 coastal forearc, Pacific coast, Costa Rica, B.S., 70 pp., Trinity Univ., San Antonio, Tex.,  
674 USA.  
675  
676 NASA (2003), 3 Arc Second SRTM Elevation Data, Shuttle Radar Topography Mission  
677 (SRTM), Jet Propulsion Laboratory (JPL), California Institute of Technology, Pasadena  
678 California, USA, v. 1.0.  
679  
680 Norabuena, E., et al. (2004), Geodetic and seismic constraints on some seismogenic zone  
681 processes in Costa Rica, *J. Geophys. Res.*, 109, B11403, doi:10.1029/2003JB002931.  
682  
683 Phillips, P. J. (1983), Stratigraphy, Sedimentology, and Petrologic Evolution of Tertiary  
684 Sediments in Southwestern Costa Rica, B.S., La. St. Univ., Baton Rouge, La., USA.  
685



686 Protti, M., et al. (1994), The Geometry of the Wadati-Benioff Zone under Southern  
687 Central-America and Its Tectonic Significance - Results from a High-Resolution Local  
688 Seismographic Network, *Phys. Earth Planet. Inter.*, 84, 271-287.  
689

690 Protti, M., et al. (1995), Correlation between the age of the subducting Cocos plate and  
691 the geometry of the Wadati-Benioff zone under Nicaragua and Costa Rica, *Spec. Paper,*  
692 *Geol. Soc. Amer.*, 295, Mann, P., 309-326.  
693

694 Protti, M., et al. (2001), Evaluación del Potencial Sísmico de la Península de Nicoya,  
695 *Fund. Univ. Nac.*, 1 ed., 144 pp.  
696

697 Ranero, C. R., et al. (2000), A cross section of the convergent Pacific margin of  
698 Nicaragua, *Tectonics*, 19, 335-357.  
699

700 Restrepo, J. F. (1987), A geochemical investigation of Pleistocene to recent calc-alkaline  
701 volcanism in western Panama, M.S., 103 pp, Univ. of South Fla., Tampa, Fla., USA.  
702

703 Shuanggen, J., and W. Zhu (2004), A revision of the parameters of the NNR-NUVEL-1A  
704 plate velocity model, *J. of Geodyn.*, 38, 85-92.  
705

706 Sak, P., et al. (2004), Effects of subducting seafloor roughness on upper plate vertical  
707 tectonism: Osa Peninsula, Costa Rica, *Tectonics*, 23, TC1017, doi:  
708 10.1029/2002TC001474.  
709

710 Shreve, R. L., and M. Cloos (1986), Dynamics of sediment subduction, mélange  
711 formation, and prism accretion, *J. Geophys. Res.*, 91, 229-245.  
712

713 Silver, E. A., et al. (1990), Implications Of The North And South Panama Thrust Belts  
714 For The Origin Of The Panama Orocline, *Tectonics*, 9, 261-281.  
715

716 Smith, W. H. F., and D. T. Sandwell, (1997) Global seafloor topography from satellite  
717 altimetry and ship depth soundings, *Science*, v. 277, p. 1957-1962.  
718

719 Tajima and Kikuchi (1995), Tectonic implications of the seismic ruptures associated with  
720 the 1983 and 1991 Costa Rica earthquakes, *Spec. Paper, Geol. Soc. Amer.*, 295, Mann,  
721 P., 327-340.  
722

723 Taylor, et al. (2005), Rapid forearc uplift and subsidence caused by impinging  
724 bathymetric features: Examples from the New Hebrides and Solomon arcs, *Tectonics*, 24,  
725 TC6005, doi 10.1029/2004TC001650.  
726

727 Vannucchi, P., et al. (2001), Tectonic erosion and consequent collapse of the Pacific  
728 margin of Costa Rica: Combined implications from ODP Leg 170, seismic offshore data,  
729 and regional geology of the Nicoya Peninsula, *Tectonics*, 20, 649-668.  
730

731 Vannucchi, P., et al. (2004), Long-term subduction-erosion along the Guatemalan margin  
732 of the middle America trench, *Geology*, 32, 617-620.  
733  
734 von Huene, R., and S. E. Lallemand (1990), Tectonic erosion along the Japan and Peru  
735 convergent margins, *Geol. Soc. Amer. Bull.*, 102, 704-720.  
736  
737 von Huene, R., and D. W. Scholl (1991), Observations at convergent margins concerning  
738 sediment subduction, subduction erosion, and the growth of continental crust, *Rev.*  
739 *Geophys.*, 29, 279-316.  
740  
741 von Huene, R., et al. (1995), Morphotectonics of the Pacific convergent margin of Costa  
742 Rica, *Spec. Paper, Geol. Soc. Amer.*, 295, Mann, P., 291-307.  
743  
744 von Huene, R., et al. (2000), Quaternary convergent margin tectonics of Costa Rica,  
745 segmentation of the Cocos plate, and Central American volcanism, *Tectonics*, 19, 314-  
746 334.  
747  
748 Werner, R., et al. (1999), Drowned 14-m.y.-old Galapagos archipelago off the coast of  
749 Costa Rica: Implications for tectonic and evolutionary models, *Geology*, 27, 499-502.  
750  
751 Yáñez, G., and J. Cembrano (2004), Role of viscous plate coupling in the late Tertiary  
752 Andean tectonics, *J. Geophys. Res.*, 109, B02407, doi: 10.1029/2003JB002494.  
753  
754 Ye, et al., (1996), Crustal structure of the Middle America trench off Costa Rica from  
755 wide-angle seismic data, *Tectonics*, 15, 1006-1021.  
756  
757 Yuan, P. B., (1984), Stratigraphy, Sedimentology, and Geologic Evolution of Eastern  
758 Terraba Trough, Southwestern Costa Rica, Ph.D., La. St. Univ., Baton Rouge, La., USA.

759

760 Figure 1. Hillshaded DEM of Central America with superimposed with tectonic  
761 boundaries and major bathymetric features. CA – Caribbean plate; PM – Panama  
762 microplate; CO – Cocos Plate; NZ – Nazca plate; NA – North American plate; ND –  
763 North Andes plate; PFZ – Panama Fracture Zone. Black box indicates boundary of

764 Figure 2. Topographic data from the SRTM30 dataset (source for this dataset is the Jet  
765 Propulsion Laboratory, <http://www2.jpl.nasa.gov/srtm/>) [NASA, 2003]. Bathymetric data  
766 from Smith and Sandwell, 1997.

767

768 Figure 2. Hillshaded DEM showing morphologic characteristics of Costa Rica and the  
769 adjacent Cocos plate. CA – Caribbean plate; PM – Panama microplate; CO – Cocos  
770 Plate; CR – Cocos Ridge; PFZ – Panama Fracture Zone; MAT – Middle America Trench;  
771 FSG – Fisher Seamount Group; QP – Quepos Plateau; FC – Fila Costeña thrust belt  
772 (black circled area). Black triangles indicate active arc volcanoes. White arrows indicate  
773 plate motion vectors relative to a fixed CA based on NNR-NUVEL-1B plate velocity  
774 model [DeMets, *et al.*, 1990; Silver, *et al.*, 1990; Shuanggen, *et al.*, 2004]. Long-dashed  
775 line represents estimated Panama microplate – Caribbean plate boundary (i.e. central  
776 Costa Rica deformed belt [Marshall, *et al.*, 2000]). Short dashed line is northward  
777 projection of PFZ. Box shows location of Figure 3. Maximum elevation is ~3800 m.  
778 Bathymetric data courtesy of GEOMAR.

779

780 Figure 3. Simplified geologic map of the southern Fila Costeña thrust belt showing fault  
781 traces, strike and dip, slickenline, and fold measurements. Stratigraphic column modified

782 from *Phillips*, [1983] and *Fisher, et al.*, [2004a]. Solid red line: Pan American highway,  
783 towns labeled, transecting the thrust belt through the Río Térraba gorge; Dashed black  
784 line: northward projection of the Panama Fracture Zone, roughly coinciding with the  
785 eastern extent of the thrust belt and the Costa Rica – Panama border; Dashed red line:  
786 onland projection of the Cocos Ridge axis; A-A': location of the cross section completed  
787 by *Fisher et al.*, [2004a]; B-B': position of the cross section completed during this study.

788

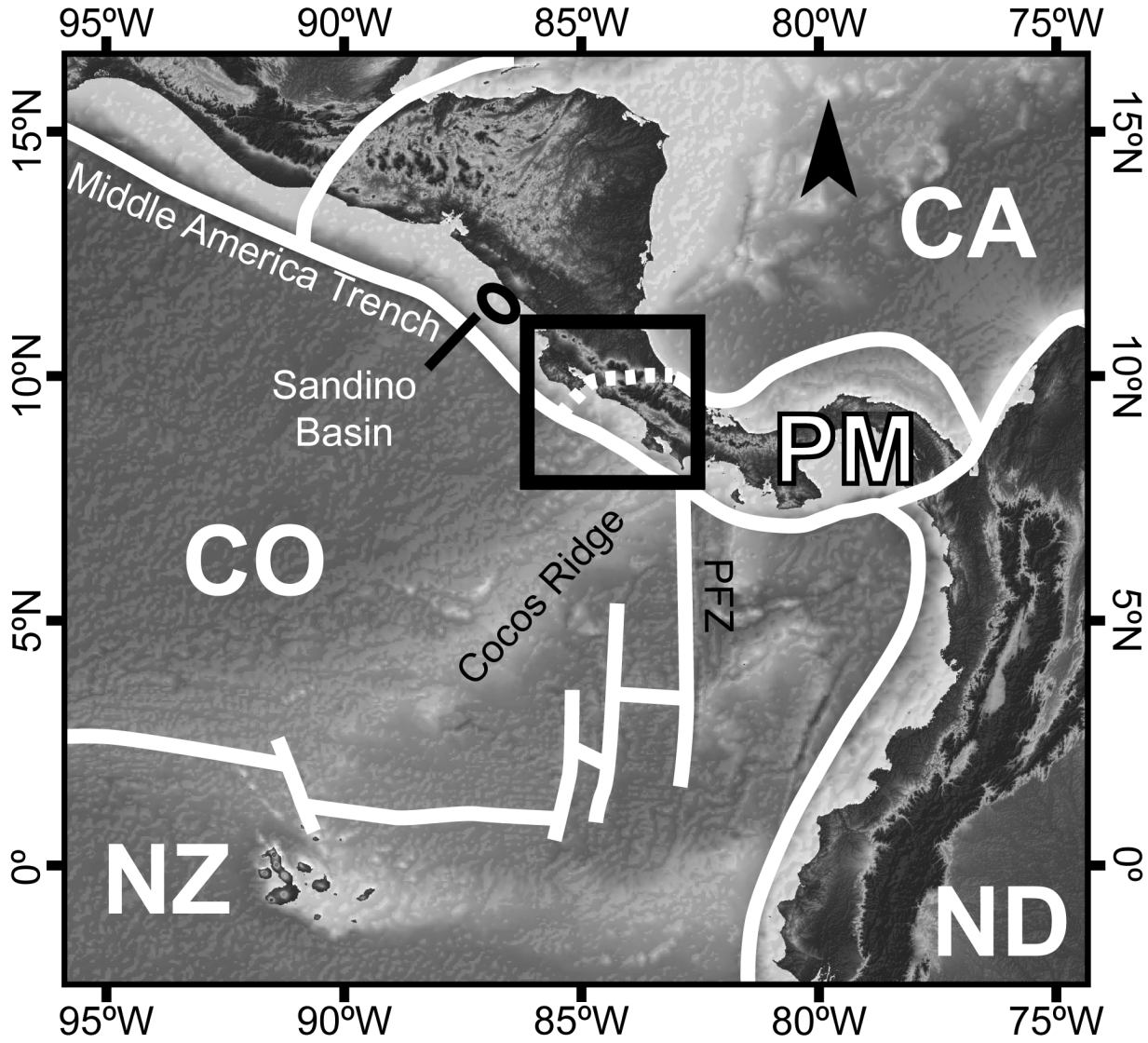
789

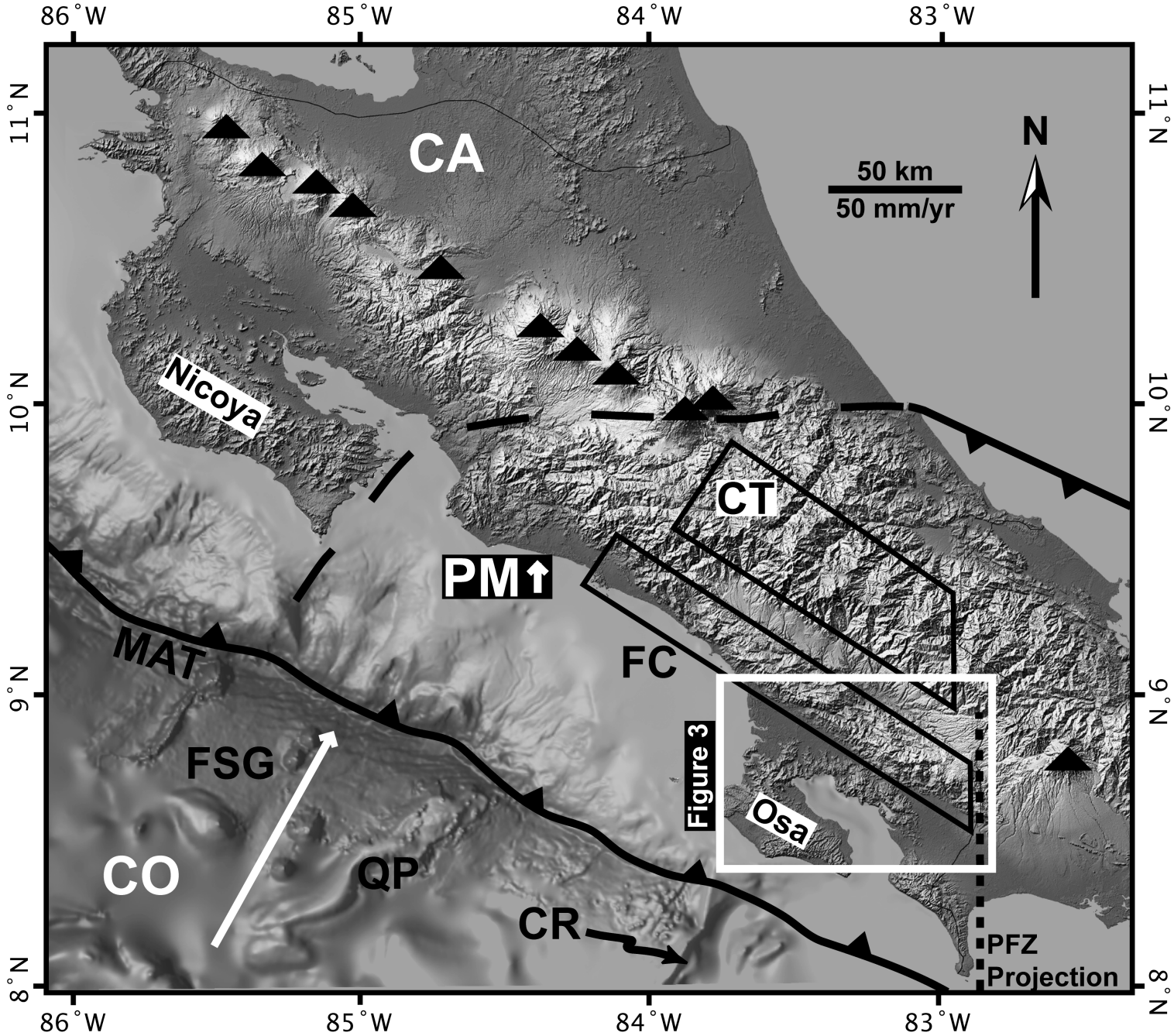
790 Figure 4. Balanced cross sections along two transects through the southern Fila Costeña  
791 thrust belt (See Figure 3 for location of sections A-A' and B-B'). Inset: Detachment depth  
792 3500 – 4000 m. Minimum depth determined by placing axial surface at rearmost dip  
793 measurement (dotted line). Short dashed line shows probable axial surface location  
794 based on total dataset. Fault ramps dip 15°-30° to the northeast. The decollément at the  
795 basement/cover contact dips 4° to the northeast. B-B' (completed during this study) lies  
796 directly inboard of the subducting Cocos Ridge axis. Minimum shortening over the five  
797 thrusts in B-B' is 36.3 km. The three frontal thrusts are horses in a duplex, and the roof  
798 thrust has been eroded. A-A' (updated from *Fisher, et al.*, [2004a]) records 17.4 km of  
799 total shortening across three thrusts. Restorations were completed by minimizing the  
800 amount of possible slip when hanging wall cutoffs were eroded. Fault #4 (previously  
801 unreported by *Fisher, et al.*, [2004a]) has been estimated and added to A-A', extending  
802 the shortened section 4.5 km and the restored section 17.4 km. No vertical exaggeration.  
803

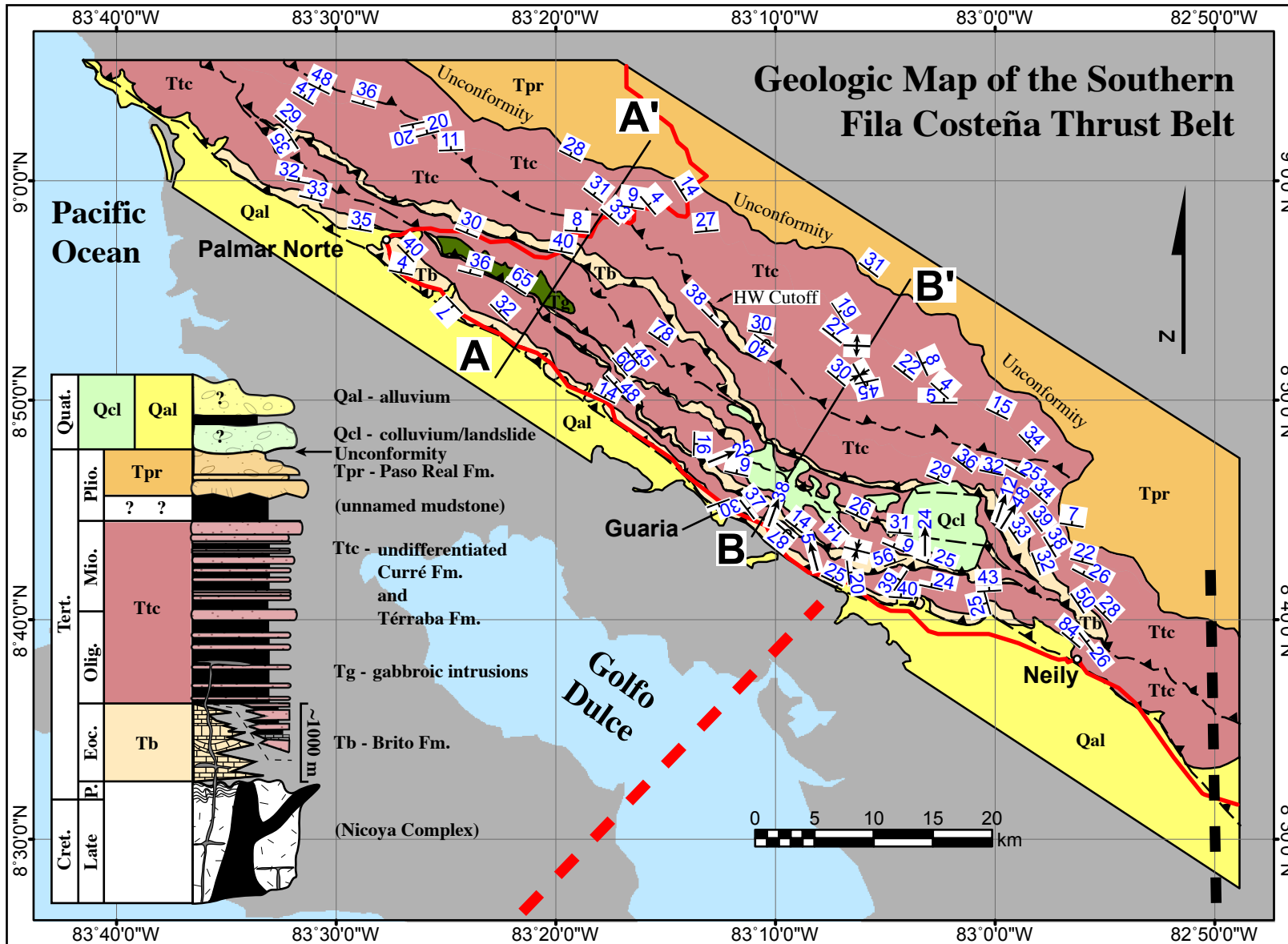
804 Figure 5. Vector diagram relating Caribbean plate (CA), Cocos plate (CO), Nazca plate  
805 (NZ), and Panama microplate (PM). Solid lines are relative plate motion vectors based  
806 on NNR-NUVEL-1B plate velocity model [DeMets, *et al.*, 1990; Silver, *et al.*, 1990;  
807 Shuanggen, *et al.*, 2004]. PM velocity estimate from Bird, [2003]. Dashed black lines  
808 represent the orientations of the Panama Fracture Zone (PFZ) and Middle America  
809 Trench (MAT) and Cocos Ridge axis (CR). Intersection of MAT and PFZ is Panama  
810 triple junction (PTJ). PTJ migrates ~55 mm/yr southeast along MAT with respect to  
811 fixed PM. Intersection of MAT and CR migrates ~20 mm/yr northwest along MAT.  
812 Thick, dashed grey lines indicate PM-NZ and PM-CO convergence rates of ~20 mm/yr  
813 and ~80 mm/yr, respectively.

814

815 Figure 6. Elevation of the Fila Costeña topographic divide plotted parallel to the margin  
816 and extending the length of the thrust belt inboard of the Cocos Ridge (~160 km). The  
817 topographic minimum in the center of the plot is the Río Terraba gorge, which transects  
818 the thrust belt. B-B' indicates position of the cross section completed in this paper  
819 (Figure 4, B-B'). Slightly southeast of this location the maximum elevation in the Fila  
820 Costeña is inboard of the subducting Cocos Ridge axis. Elevation of the divide decreases  
821 rapidly toward the onland projection of the Panama Fracture Zone.









SW

NE

